Testing Climate Models Using Infrared Spectra and GNSS Radio Occultation

S. S. Leroy[1], **J. A. Dykema**[1], **P. J. Gero**[1], **and J. G. Anderson**[1]

Harvard School of Engineering and Applied Sciences, Harvard University, Cambridge, Massachusetts, U.S.A.
leroy@huarp.harvard.edu

Abstract The Climate Absolute Radiance and Refractivity Observatory will be a climate benchmarking mission intended to include instruments for measuring Earth's atmospheric refractivity by GNSS radio occultation (RO), high spectral resolution thermal infrared spectra emitted from the Earth, and the spectrally resolved reflected shortwave spectrum. Climate benchmarking is necessary to establish a record that can be used to test climate models according to their predictive capability because other attempts at establishing trustworthy timeseries of satellite data have not been particularly successful. We have investigated how GNSS RO measurements and thermal infrared spectra can be used to test models' predictive capability. GNSS RO provides a constraint on the transient sensitivity of the climate system. Infrared radiance spectra can quantify the individual longwave feedbacks of the climate system, including cloud-longwave feedbacks when used in conjunction with GNSS RO. At present, studies are limited to clear sky infrared radiation, so the next research steps should include cloudy sky infrared simulations and reflected shortwave simulations.

1 Introduction

The Decadal Survey of the U.S. National Oceanic and Atmospheric Administration (NOAA) and the U.S. National Aeronautics and Space Administration (NASA) by the U.S. National Research Council (NRC) recommended that NASA deploy a Climate Absolute Radiance and Refractivity Observatory (CLARREO) as one of its four highest priorities. This recommendation came in response to a request from NASA and NOAA to suggest what satellite missions should be flown to form a national climate research program that is responsive to societal demands (National Research Council, Committee on Earth Science and Applications from Space 2007). Society demands data sets deemed trustworthy for trend detection and sufficiently accurate to test climate models according to their predictive capability, and for this reason the U.S. NRC recommended the CLARREO mission to NASA as a top priority. In short, society needs tools that usefully predict future climates depending on

its own decisions regarding future economic development and energy production. Those tools are climate models and, pursuant to the scientific paradigm, must be tested empirically.

CLARREO calls for three instruments: a GNSS (global navigation satellite system) occultation instrument, an instrument to measure emitted infrared radiation with high spectral resolution, and an instrument to measure reflected shortwave radiation with high spectral resolution. In order to ensure their data are absolutely accurate, it is required that they are assured traceable to the international standards that define the units of their observables on-board with overall uncertainties sufficient to test climate models (Ohring 2007). It is also required that their sampling patterns be sufficiently dense and uniform so that mission accuracy requirements are met. The optimal configuration for monitoring the emitted infrared spectrum with three satellites has them in perfectly polar orbits (90° inclination) spaced 60° in longitude of ascending node (Kirk-Davidoff et al. 2005). Such a configuration affords robustness in that the bias in annual averages induced by the diurnal cycle would be minimal should one or two satellites fail. Should all three satellites be operational, bias in *seasonal* averages induced by the diurnal cycle would be minimized.

The data types called for by CLARREO were selected because their traceability to international standards is possible. The NRC Decadal Survey's recommendation should answer societal demands, which in this case pertain to testing climate models. In what ways the data types of CLARREO can be used to test climate models according to their predictive capability remains an open question. In testing climate models, the scientific assessments of the Intergovernmental Panel on Climate Change focus much of their efforts in comparing the overall sensitivities of climate models, which is the surface air temperature increase predicted by a climate model when subjected to a prescribed forcing by increased carbon dioxide. Certainly, the sensitivity of the climate system must be modeled correctly, but a trustworthy model must attain the correct sensitivity for the right physical reasons. There are many ways to explain the sensitivity of a climate model (and the actual climate system), and, for the sake of simplicity, we analyze the sensitivity in the language of radiative feedbacks.

2 Radiative feedbacks

The climate's greenhouse effect comes about because of the presence of well-mixed gases that absorb efficiently in the thermal infrared while the same atmosphere is largely transparent at visible wavelengths where most of the solar forcing occurs. The shortwave radiative forcing occurs largely at the Earth's surface, and the surface cannot easily cool itself by radiating to space in the thermal infrared because of the greenhouse gases present. As a consequence, the surface has to warm more to maintain a radiative balance than it would have without the greenhouse gases present.

It is possible for some elements of the atmosphere to respond to surface temperature change in such a way that radiation from the troposphere is either enhanced or suppressed. When temperature increases and thermal infrared (longwave) radiation from the troposphere is partially suppressed, the action is considered a *positive* radiative feedback; when temperature increases and longwave radiation from the troposphere is enhanced, the action is considered a *negative* radiative feedback.

An injection of anthropogenic greenhouse gases, before anything else happens, has the immediate effect of blocking photons from escaping the troposphere. The amount of radiation flux blocked is called a radiative forcing ΔF_{rad}. To first order, the surface responds by increasing its temperature by an amount $\Delta T^{(1)}$, thus increasing the flux through the tropopause and restoring radiative balance. The statement is

$$\Delta T^{(1)} = \frac{\Delta F_{\text{rad}}}{\Gamma} \tag{1}$$

in which $\Gamma \approx 4\varepsilon\sigma T^3$ is the gray-body radiation term for the surface, ε a combination of surface emissivity and the fraction of radiation from the surface that escapes to space, and σ the Stefan-Boltzman constant. The climate system responds dynamically and thermodynamically to such a surface temperature change, and some of those reactions act to enhance radiation to space and some to suppress it. A continuum of such feedbacks exists, a geometric series for surface temperature change results, and the final surface temperature change is

$$\Delta T = \Delta F_{\text{rad}} \left(\Gamma - \sum_i \gamma_i^{\text{LW}} - \sum_i \gamma_i^{\text{SW}} \right)^{-1} \tag{2}$$

where the longwave feedback factors γ_i^{LW} and shortwave feedback factors γ_i^{SW} are defined by

$$\begin{aligned} \gamma_i^{\text{LW}} &= \left(\frac{\partial F^{\text{LW}}}{\partial x_i}\right) \frac{dx_i}{dT} \\ \gamma_i^{\text{SW}} &= \left(\frac{\partial F^{\text{SW}}}{\partial x_i}\right) \frac{dx_i}{dT} \end{aligned} \tag{3}$$

where F^{LW} is the net downward longwave flux at the tropopause, F^{SW} is the net downward shortwave flux at the tropopause, and x_i can be any one of a long list of meteorological, thermodynamic, or constituent properties that can affect longwave or shortwave radiation. A positive feedback has $\gamma > 0$, and a negative feedback has $\gamma < 0$. The largest feedbacks are thought to be the water vapor-longwave feedback, the cloud-shortwave feedback, the upper tropospheric temperature-longwave ("lapse rate") feedback, and the hypothesized aerosol indirect effects in the shortwave. The most uncertain feedbacks are thought to be the cloud-shortwave feedback and the aerosol indirect effect. This calculus of feedbacks has been presented elsewhere (Cess 1976; Wetherald and Manabe 1988) as have reviews about feedbacks implicit in climate models (Held and Soden 2000; Colman 2003; Bony et al. 2006; Soden and Held 2006).

3 Testing feedbacks with CLARREO

If climate models accurately reproduce climate sensitivity, one way to ascertain whether they do so for the correct physical reasons is to divide climate response according to feedbacks. CLARREO should be capable of doing so because individual feedbacks have distinctive spectral signatures in the thermal infrared and visible wavelengths. GNSS occultation should play an important role because of its insensitivity to clouds: it might resolve the cloud-surface temperature ambiguity inherent to sounding in the thermal infrared. We apply optimal fingerprinting techniques to spectral infrared and microwave refractivity as produced offline by many sophisticated climate models. This should tell us the relative contribution of various data types to testing various climate feedbacks, what accuracy is needed for each data type, and how long we should expect to wait before a satisfactory test can be applied to climate models' predictions.

A feedback can be determined by trend analysis by dividing the trend in outgoing radiation due to a specific thermodynamical variable or constituent concentration by the trend in surface air temperature:

$$\gamma_i^{\mathrm{LW}} = \frac{dF_i^{\mathrm{LW}}}{dt}\left(\frac{dT}{dt}\right)^{-1} \tag{4}$$

with dF_i^{LW} the change in downward radiation at the tropopause due to a change in thermodynamic variable or constituent concentration i. In order to estimate the feedback, one must be able to estimate dF_i^{LW}/dt observationally as well as dT/dt. Moreover, observations in the thermal infrared allow one to detect radiative forcing by anthropogenic greenhouse gases, ΔF_{rad}. [Presently, an exploration of the possibility of testing climate models has been done only for longwave radiation and not yet for shortwave radiation; hence, we restrict our discussion to the longwave.]

If a variable perturbs the tropopause radiation field, then it has an associated feedback, and because changes in variables lead to unique changes in the infrared spectrum at the tropopause, careful observation of the evolution of the tropopause radiation field should constrain the feedbacks of the climate system. In fact, in most cases individual feedbacks have unique fingerprints in the spectra of outgoing longwave and shortwave radiation. CLARREO, in measuring the outgoing longwave radiation, can uniquely discern the longwave feedbacks because each has a unique signature in the thermal infrared spectrum. How long a timeseries of CLARREO-like data is necessary before climate models' realizations of the climate feedbacks can be tested remains an open question.

In Fig. 1 we show the spectral infrared signatures of tropospheric temperature change, stratospheric temperature change, tropospheric water vapor increase, and carbon dioxide increase. Because water vapor inhibits outgoing longwave radiation with time, as can be seen by the sign of the integral of its signal over frequency in Fig. 1, it is associated with a positive longwave feedback. In clear skies, we seek to model the trend in the emitted infrared spectrum as a linear combination of these four signals while allowing for some uncertainty in the modeled shape of these sig-

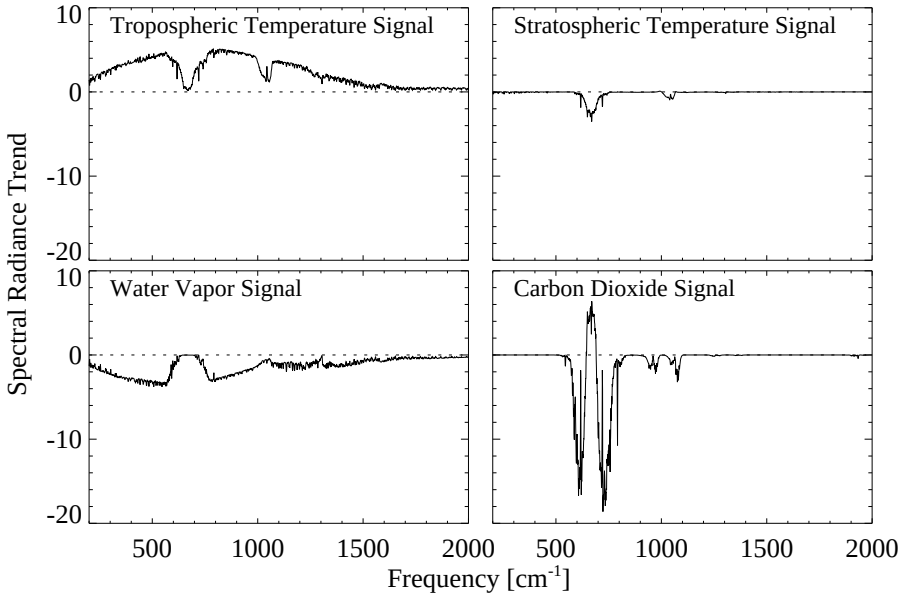

Fig. 1 Spectral infrared signals corresponding to calculus of feedbacks. The tropospheric temperature signal shows how the troposphere cools itself; the carbon dioxide signals shows the spectral fingerprint of radiative forcing by carbon dioxide; the water vapor signal shows the spectral fingerprint of the water vapor-longwave feedback. The units for the radiance trend for all plots in this figure are W cm^{-2} (cm^{-1})$^{-1}$ sr^{-1} decade^{-1}.

nals. The quality of the eventual fit is measured against the natural variability in the emitted infrared spectrum on interannual time scales. The mathematical technique is just the same as that used in climate signal detection and attribution studies (Allen et al. 2006) with an allowance for signal shape uncertainty (Huntingford et al. 2006). The "model" for the linear trend in the emitted infrared spectrum $d\mathbf{d}/dt = dF_\nu^{\mathrm{LW}}/dt$ is

$$\frac{d\mathbf{d}}{dt} = \sum_i \left(\frac{d\alpha_i}{dt}\right)\mathbf{s}_i + \frac{d}{dt}\delta\mathbf{n} \tag{5}$$

where the $\mathbf{s}_i$ are the spectral shapes given in Fig. 1, the $d\alpha_i/dt$ are scalar estimators of the trends of outgoing longwave radiation associated with individual variables, and the $\delta\mathbf{n}$ are realizations of interannual variability in the tropics (30°S to 30°N) as they would appear in the annual average emitted infrared spectrum. The solution for the trend estimators $d\alpha_i/dt$ is given by

$$\frac{d\alpha}{dt} = \mathbf{F}^T \frac{dF_\nu^{\mathrm{LW}}}{dt} \tag{6}$$

where the columns of the matrix $\mathbf{F}$ are the components of the contravariant basis to the fingerprint basis established by the $\mathbf{s}_i$. As a consequence, $\mathbf{F}^T\mathbf{S} = \mathbf{I}$ where the

columns of $\mathbf{S}$ are the $\mathbf{s}_i$, and so we call $\mathbf{F}$ the set of contravariant fingerprints. Consistent with Bayesian inference (Leroy 1998), optimal methods (Bell 1986; North et al. 1995), and a geometric approach (Hasselmann 1997), the contravariant fingerprints are given by

$$\mathbf{F} = \Sigma^{-1}\mathbf{S}(\mathbf{S}^T\Sigma^{-1}\mathbf{S})^{-1} \tag{7}$$

where Σ is a covariance matrix describing the statistics of natural variability and uncertainty in the shapes $\mathbf{s}_i$:

$$\Sigma = \Sigma_{d\mathbf{n}/dt} + \Sigma_{\mathbf{S}}. \tag{8}$$

The contributions of natural variability and signal uncertainty must be evaluated differently because of their different natures. Natural variability influences a measured trend in the emitted infrared spectrum simply because any timeseries of a random phenomenon yields a nonzero residual trend. If the covariance of natural variations in the annual average emitted infrared spectrum is $\Sigma_{\delta\mathbf{n}}$, then for serially uncorrelated variability the residual trend has zero expected mean but an uncertainty of $\Sigma_{d\mathbf{n}/dt}$:

$$\Sigma_{d\mathbf{n}/dt} = \frac{12\tau}{(N^3-N)(\mathrm{yr}^3)}\,\Sigma_{\delta\mathbf{n}} \tag{9}$$

where N is the number of years in the continuous timeseries and $\tau = 1$ yr for no serial correlation (see Eqs. 6 and 7 in Leroy et al., 2008b). The covariance of natural interannual variability is evaluated using a long control run of a climate model in conjunction with a forward model for emitted infrared spectrum. On the other hand, the covariance of signal shape uncertainty must be evaluated using a large ensemble of climate models each of which can be used to determine its own set of signal shapes $\mathbf{s}_i$. Because we are interested in trends of spectrally integrated outgoing longwave radiation, for each model used to derive $\mathbf{s}_i$, the signals are normalized such that the spectral integral of $\mathbf{s}_i$ multiplied by π (to account for integration over solid angle) is unity. Then the signal shape uncertainty covariance is

$$\Sigma_{\mathbf{S}} = \sum_{i,j}\left(\frac{d\alpha_i}{dt}\right)\left(\frac{d\alpha_j}{dt}\right)\langle \mathbf{s}_i\,\mathbf{s}_j^T\rangle \tag{10}$$

where the $\langle\cdots\rangle$ denotes an ensemble average over a large number of models and the $d\alpha_i/dt$ are prior estimates of the trend in outgoing longwave radiation associated with signal i. The contravariant fingerprints are then obtained by substituting the expressions for $\Sigma_{d\mathbf{n}/dt}$ and $\Sigma_{\mathbf{S}}$ in Eqs. 9 and 10 into Eq. 8 and in turn into Eq. 7. When the contravariant fingerprints are multiplied by annual average infrared spectral anomalies, the result will be the outgoing longwave radiation (OLR) anomalies associated with the prescribed feedbacks.

Ordinary error estimation (for just one signal $\mathbf{s}$ instead of multiple signals $\mathbf{S}$) dictates that the posterior uncertainty covariance for the OLR trends associated with the feedbacks should be

$$\sigma^2_{d\alpha/dt} = (\mathbf{s}^T\Sigma^{-1}\mathbf{s})^{-1} \tag{11}$$

but too often prescriptions of natural variability are grossly different from reality. Consequently, a better estimate of the posterior error should be obtained from the data alone. This is done by ordinary linear regression on a detector timeseries $\alpha(t)$ (c.f. Eq. 15 below). With the timeseries $\alpha(t)$, the error is determined first by estimating the natural variability in the detectors which is the variance of the $\alpha(t)$ after removal of a best linear fit $\alpha_{\rm fit}(t)$. The uncertainty in the trend $d\alpha/dt$ due to natural variability becomes

$$\sigma^2_{d\alpha/dt}(\text{natural variability}) = \frac{\sigma^2_\alpha}{N\,(\Delta t)^2} \tag{12}$$

where $(\Delta t)^2 = \sum_{i=1}^N (t_i - \bar{t})^2/N$ is the variance of the coordinate times in the timeseries. The timeseries $\alpha(t)$ contains only variability related to natural variability and no uncertainty due to signal shape uncertainty, so the latter must be added separately. By standard error propagation techniques,

$$\sigma^2_{d\alpha/dt}(\text{signal shape}) = \mathbf{F}^T \boldsymbol{\Sigma}_{\mathbf{s}} \mathbf{F} \tag{13}$$

and thus the error in the forecast trend is

$$\sigma^2_{d\alpha/dt} = \sigma^2_{d\alpha/dt}(\text{natural variability}) + \sigma^2_{d\alpha/dt}(\text{signal shape}). \tag{14}$$

If natural variability were correctly prescribed by that used in composing the contravariant fingerprint $\mathbf{F}$, then $\sigma^2_{d\alpha/dt}(\text{natural variability}) = \mathbf{F}^T \boldsymbol{\Sigma}_{d\mathbf{n}/dt} \mathbf{F}$ and the result becomes exactly that in Eq. 11.

To demonstrate the viability of this approach to linear regression, we have computed the contravariant fingerprints $\mathbf{F}$ using the output of several models of the World Climate Research Programme's (WCRP's) Coupled Model Intercomparison Project (CMIP3) multi-model data set, subjected to SRES-A1B forcing. Case A1B of the Special Report on Emission Scenarios (SRES) predicts radiative forcing of climate in a world of rapid economic growth, rapid technological growth, increasing social interaction, and decelerating population growth (Intergovernmental Panel on Climate Change (IPCC) 2000). It features approximately 1% yr^{-1} CO_2 increase to $\approx$ 720 ppm and radiative forcing by sulfate aerosols peaking in year $\approx$ 2020. We take annual averages of emitted infrared spectra based on monthly average output and average over the tropics. The signals $\mathbf{s}_i$ are estimated based on the first 50 years of output. We then computed 20 years of emitted infrared spectra from a climate model independent of those used to construct the contravariant basis. We multiplied the contravariant fingerprints by tropical average, annually averaged emitted infrared spectra from that climate model. The result is a timeseries of detectors $\alpha(t)$:

$$\alpha(t) = \mathbf{F}^T \mathbf{d}(t). \tag{15}$$

The result is shown in Fig. 2. In both the "truth" (open squares) and analysis (solid squares) there is variability from year to year. This variability contributes in large part to the length of time required to elapse before useful climate model testing can

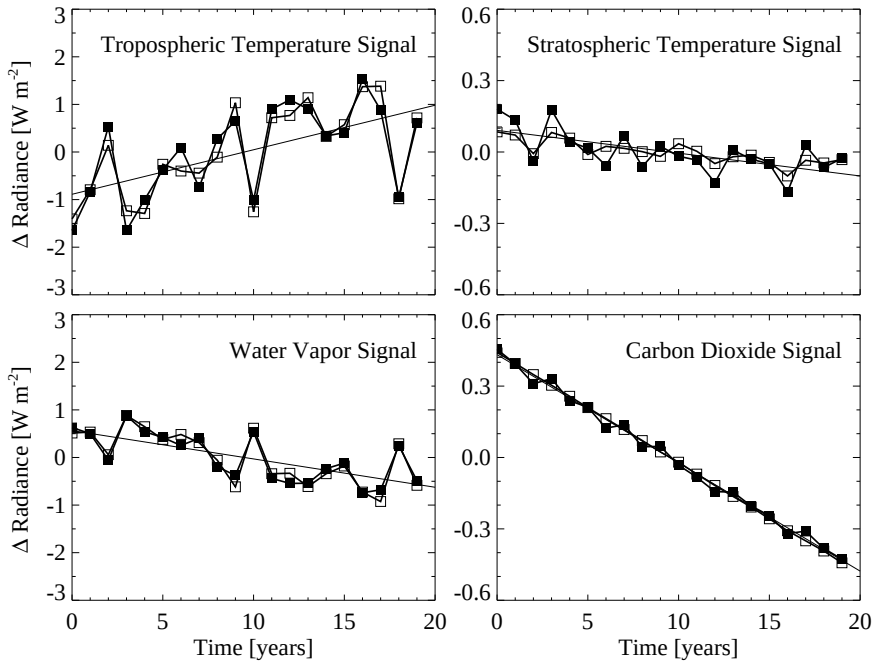

Fig. 2 Detection amplitude timeseries for four signals. The solid squares show detection amplitudes for each of four detected signals and the open squares show true OLR anomalies for each of the four signals. The thin solid line is the best linear fit to the detection amplitudes. The "truth" data set is taken from the first 20 years of output of an SRES-A1B run of GFDL CM2.1.

take place. In the case of greenhouse forcing by carbon dioxide, it is evident from the small fluctuations associated with interannual variability that direct observation of anthropogenic *radiative forcing* of the climate should be detected and strongly constrained within just a few years. After 5 years of observation, in fact, an estimate of radiative forcing by carbon dioxide with just 20% uncertainty should be obtained. Detection of tropospheric temperature trends (climate response) and longwave suppression by water vapor requires more time because of the large fluctuations associated with interannual variability. After 20 years of observation, an estimate of the water vapor-longwave feedback in the tropics with $\sim 50\%$ uncertainty can be obtained by trend analysis.

Fig. 2 suggests a different analysis as well. The year to year anomalies of the tropospheric temperature and water vapor signals are strongly anticorrelated. This is related to the simple fact that tropical tropospheric water vapor increases and blocks surface radiation in years when the tropical troposphere is warm following the Clausius-Clapeyron equation. The slope of this correlation then can be used to estimate the water vapor-longwave feedback. In fact, such an *anomaly correlation* analysis can be used to estimate the water vapor-longwave feedback in the tropics with 7% uncertainty in ten years. The uncertainty scales as $(\Delta t)^{-1/2}$ for anomaly

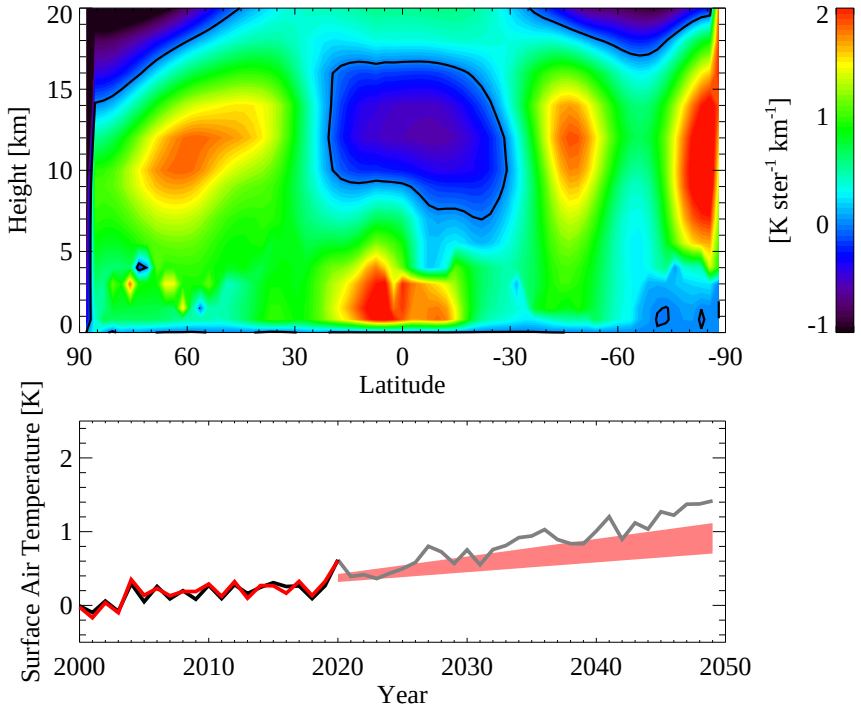

Fig. 3 The top plot shows the contravariant fingerprint (**F**) for log-dry pressure as an indicator of surface air temperature trends. The lower plot shows the result of the application of this approach using detectors, with a 20-yr timeseries of dry pressure "data" taken from the output of a model not used in the construction of the contravariant fingerprint. The black curve shows actual global average annual average surface air temperature, and the red curve shows the detectors $\alpha(t)$. The red-shaded area from years 2020 to 2050 show the forecast trend of surface air temperature based on the simulated upper air dry pressure data from 2000 to 2020, and the gray curve shows the actual evolution of the surface air temperature.

correlation analysis whereas the uncertainty scales as $(\Delta t)^{-3/2}$ for trend analysis, with Δt the time baseline of the continuous timeseries of data.

Actual spectral longwave data, though, are dominated by clouds, and thus the use of GNSS radio occultation (RO) is likely to be necessary. Leroy et al. (2006) have shown that the optimal fingerprint of climate change in upper air *dry pressure*—dry pressure is the atmospheric pressure derived from GNSS RO data under the assumption of a completely dry atmosphere—is poleward migration of the mid-latitude jet streams in both the Northern and Southern Hemispheres. In Fig. 3 we show the results of the application of the methodology described by Eqs. 6 through 9 when applied to zonal average, annual average log-dry pressure (instead of infrared spectra F_ν^{LW}) as might be obtained from GNSS RO data normalized by the surface air temperature trend dT/dt.

The contravariant fingerprint **F** and the detector timeseries $\alpha(t)$ are used to infer past and predict future surface air temperature trends given zonal average, annual average log-dry pressure data from GNSS RO only. The contravariant fingerprint is the map by which one convolves the trends in data to obtain a trend in surface air temperature:

$$\frac{dT}{dt} = \langle \mathbf{F}, \frac{d\mathbf{d}}{dt} \rangle = \frac{d}{dt} \langle \mathbf{F}, \mathbf{d}(t) \rangle = \frac{d}{dt} \alpha(t) \tag{16}$$

(c.f. Eq. 15). The inner product rule in this case is

$$\langle \mathbf{a}, \mathbf{b} \rangle = \int_{-\pi/2}^{\pi/2} 2\pi \, d(\sin\theta) \int_{0 \text{ km}}^{20 \text{ km}} dh \, a(\theta, h) \, b(\theta, h) \tag{17}$$

where θ is latitude and h is height, the coordinates of the map. The contravariant fingerprint has dimensions of surface air temperature per log-dry pressure per height interval per solid angle interval on the Earth's surface. The intervals are determined by the data grid. The slope of the detector timeseries is used to infer and predict the surface air temperature trend and its related uncertainty.

As can be seen in Fig. 3, when upper air log-dry pressure is used as an indicator of trends in surface air temperature, the fingerprint searches for poleward migration of the mid-latitude jet streams, a tropical contribution that involves subtraction of upper tropospheric temperature trends from lower tropospheric humidity trends, and a possible weakening of the southern stratospheric polar vortex. Poleward migration of the mid-latitude jet streams is the leading indicator of climate change in the tropospheric upper air (Leroy et al. 2006). In this application, the detectors capture the interannual fluctuations of global average surface temperature with accuracy < 0.1 K, meaning GNSS RO can be relied upon to obtain an accurate estimate of the dT/dt that is necessary for estimating radiative feedbacks. This is an improvement over the use of *in situ* meteorological stations which are largely restricted to land.

4 Discussion

We have described how monitoring the emitted infrared spectrum and microwave refractivity using GNSS RO can be used to test the forecasting capability of climate models. The infrared spectrum is rich in information relevant to the longwave feedbacks of the climate system and microwave refractivity contains information relevant to the response of the upper air and surface air temperature. Leroy et al. (2008a) showed that a twenty year timeseries of longwave spectral data is expected to provide a 50% uncertain estimate of the water vapor-longwave feedback of the climate system and a 20% uncertain estimate of the longwave forcing by carbon dioxide in 5 years. Anomaly correlation is expected to work well in the tropics on an annual timescale because temperature and humidity are strongly coupled in the tropical troposphere by moist convection. Whether it can be expected to work in the mid- and high latitudes remains an open question, however.

An evaluation of the longwave feedbacks by trend analysis can only be obtained with a corresponding accurate estimate of the trend in global average surface air temperature. Accurate estimation of the global average surface air temperature is expected to be complicated by the evolution of low clouds. Their infrared spectral signatures are very similar, and a small amount of error that might result from this ambiguity would significantly influence an evaluation of the longwave feedbacks, especially a low cloud-longwave feedback. For this reason, microwave refractivity as obtained by GNSS RO has a valuable role to play. Microwave refractivity is mostly insensitive to clouds, and so it can be expected to resolve a low cloud-temperature ambiguity in trends in the emitted infrared spectrum. Leroy et al. (2006) showed that the leading indicator of climate change in upper air dry pressure is poleward migration of the mid-latitude jet streams. Generalized scalar prediction shows that surface air temperature prediction can be obtained by poleward migration of the mid-latitude jet streams as well. The resulting analysis for dT/dt is more uncertain than simple measurements of surface air temperature trends because of the influence of natural variability in the upper air, but satellite data does not suffer from the same coverage problems as does *in situ* data.

The future direction in this line of research quite obviously points toward simulations using cloudy outgoing longwave spectra. Clouds are acknowledged to be associated with the most uncertain feedbacks. Only recently have climate models published output relevant to simulating cloudy longwave radiances. Once clouds are included in the simulation of emitted infrared spectra, the surface temperature-low cloud ambiguity is introduced. The surface temperature-low cloud ambiguity in outgoing longwave spectra and the wet-dry ambiguity in microwave refractivity might both be resolved by considering outgoing longwave spectra and microwave refractivity jointly in climate model testing and optimal fingerprinting. Such a joint detection should be accomplished by expanding the proposed data vector to include multiple data types and computing signals and natural variability accordingly.

Finally, the cloud-shortwave feedbacks remain the most uncertain feedbacks implicit in climate models, so an exploration of how climate models can be tested using reflected shortwave (visible) spectra is mandatory for responding to societal demands.

Acknowledgments. We acknowledge the modeling groups, the Program for Climate Model Diagnosis and Intercomparison (PCMDI) and the WCRP's Working Group on Coupled Modelling (WGCM) for their roles in making available the WCRP CMIP3 multi-model dataset. Support of this dataset is provided by the Office of Science, U.S. Department of Energy. This work was supported by grant ATM-0450288 of the U.S.National Science Foundation.

References

Allen M, Gillett N, Kettleborough J, Hegerl G, Schnur R, Stott P, Boer G, Covey C, Delworth T, Jones G, Mitchell J, Barnett T (2006) Quantifying anthropogenic influence on recent near-surface temperature change. Surv Geophys 27:491–544

Bell T (1986) Theory of optimal weighting to detect climate change. J Atmos Sci 43:1694–1710

Bony S, Colman R, Kattsov V, Allan R, Bretherton C, Dufresne J, Hall A, Hallegatte S, Holland M, Ingram W, Randall D, Soden B, Tselioudis G, Webb M (2006) How well do we understand and evaluate climate change feedback processes? J Climate 19:3445–3482

Cess R (1976) Climate change—Appraisal of atmospheric feedback mechanisms employing zonal climatology. J Atmos Sci 33(10):1831–1843

Colman R (2003) A comparison of climate feedbacks in general circulation models. Climate Dyn 20:865–873

Hasselmann K (1997) Multi-pattern fingerprint method for detection and attribution of climate change. Climate Dyn 13(9):601–611

Held I, Soden B (2000) Water vapor feedback and global warming. Ann Rev of Energy and Env 25:441–475

Huntingford C, Stott P, Allen M, Lambert F (2006) Incorporating model uncertainty into attribution of observed temperature change. Geophys Res Lett 33:doi:10.1029/2005GL024831

Intergovernmental Panel on Climate Change (IPCC) (2000) Special Report on Emissions Scenarios. Cambridge University Press, Cambridge, U.K.

Kirk-Davidoff D, Goody R, Anderson J (2005) Analysis of sampling errors for climate monitoring satellites. J Climate 18(6):810–822

Leroy S (1998) Detecting climate signals: Some Bayesian aspects. J Climate 11(4):640–651

Leroy S, Anderson J, Dykema J (2006) Testing climate models using GPS radio occultation: A sensitivity analysis. J Geophys Res 111:D17105, doi:10.1029/2005JD006145

Leroy S, Anderson J, Dykema J, Goody R (2008a) Testing climate models using thermal infrared spectra. J Climate, in press

Leroy S, Anderson J, Ohring G (2008b) Climate signal detection times and constraints on climate benchmark accuracy requirements. J Climate 21(4):841–846

National Research Council, Committee on Earth Science and Applications from Space (2007) Earth Science and Applications from Space: National Imperatives for the Next Decade and Beyond. National Academies Press, Washington, D.C.

North G, Kim K, Shen S, Hardin J (1995) Detection of forced climate signals: I. Filter theory. J Climate 8(3):401–408

Ohring G (ed) (2007) Achieving Satellite Instrument Calibration for Climate Change. National Oceanographic and Atmospheric Administration, Washington, D.C.

Soden B, Held I (2006) An assessment of climate feedbacks in coupled ocean-atmosphere models. J Climate 19(14):3354–3360

Wetherald R, Manabe S (1988) Cloud feedback processes in a general circulation model. J Atmos Sci 45(8):1397–1415